

Final Report
Paleoseismology and Seismic Hazards of
the San Cayetano Fault Zone

02HQGR0041

James F. Dolan
Department of Earth Sciences
University of Southern California
Los Angeles, CA
90089-0740
(213) 740-8599
dolan@earth.usc.edu

Southern California (SC)
Key Words: Neotectonics, Trench Investigations, Paleoseismology, Recurrence Interval

Introduction and Rationale for Research: The San Cayetano Fault

The San Cayetano fault is a major, north-dipping reverse fault that extends for 40 km along the northern edge of the Ventura Basin and westward into the Sespe Mountains (Figure 1). The fault has been mapped in detail both at the surface and in the subsurface by a number of researchers, including Schlueter (1976), Yeats (1983), Çemen (1977; 1989), Dibblee (1987, 1990a, 1990b, 1991), Rockwell (1988), Yeats et al. (1994), and Huftile and Yeats (1995a; 1995b; 1996). These studies reveal that the San Cayetano fault is separated into two major sections (or 'lobes') by the 4-km-wide, Sespe Creek lateral ramp near the city of Fillmore (Figure 2). The eastern, or 'Modelo' lobe (so named because of prominent exposures of the Miocene Modelo Formation mudstone in the hanging wall), reaches the surface near the southern edge of the mountain front (Figure 3). The surface trace of the fault dies out ~1 km east of the city of Piru, near the mouth of Piru Creek. The mechanical connection between the San Cayetano fault and the Santa Susana fault--the major, high-slip-rate north-dipping reverse fault to the east -- is structurally complicated, and there does not appear to be a simple, through-going mechanical connection between these two faults (Yeats, 1987; Huftile and Yeats, 1996). The western 'lobe' of the San Cayetano fault differs markedly in character from the eastern lobe. The surface trace of the western lobe lies well above the base of slope of the Sespe Mountains, indicative of the fact that the western San Cayetano fault is underlain by the active, south-dipping Sisar blind thrust fault system (Huftile and Yeats, 1995a).

Global Positioning System (GPS) geodetic studies of the Ventura Basin indicate that the basin is shortening in a north-south direction at a rate of ~7 mm/yr (Donnellan et al., 1993a; 1993b); a model that incorporates the behavior of the thick, compliant sediments of the deep Ventura basin suggests slightly faster convergence rates on the order of 8–12 mm/yr (Hager et al., 1999). This shortening is accommodated by reverse slip along the north-dipping San Cayetano fault and the south-dipping Oak Ridge fault, which extends along the southern edge of the basin (see Suppe and Medwedeff [1990] and Yeats [1993] for alternative interpretations of the subsurface geometry of the Oak Ridge fault).

Structural modeling and analysis of petroleum industry data from the Hopper Canyon oil field 5 km east of Fillmore suggest that most of the shortening occurs along the San Cayetano fault (Figure 3; Huftile and Yeats, 1996). Using petroleum industry well and seismic reflection data, Huftile and Yeats (1996) estimated that the San Cayetano fault has accommodated at least 7.5 km, and possibly ~10-12 km, of shortening across an ~1 million year-old datum, yielding an average, best-estimate reverse-slip rate over the past million years of ~10-12 mm/yr. If the maximum average long-term slip rate is reflective of the current slip rate, correction for the 30° dip of the fault would yield a best-estimate north-south horizontal shortening rate of ~7-8 mm/yr (Huftile and Yeats, 1996), suggesting that most shortening across the Ventura Basin is now accommodated by the San Cayetano fault in the region of Hopper Canyon. The very rapid reverse-slip rate for the eastern San Cayetano fault (the fastest of any known reverse fault in California south of the Cascadia subduction zone) suggests that the San Cayetano fault produces either very large, or very frequent earthquakes (or both). Slip rates on the western lobe are

slower than the eastern lobe, ranging from ~1.5 to 5.5 mm/yr, decreasing westward, and dying off to zero where the surface trace of the fault ends just east of the city of Ojai (Figure 1) (Rockwell, 1988).

Thus, the San Cayetano fault, and in particular the eastern 'Modelo' lobe of the fault, exhibits one of the fastest slip rates of any fault in California, and it may be capable of producing very large earthquakes. Dolan et al. (1995) identified the San Cayetano fault as one of six major fault systems within the greater Los Angeles metropolitan region potentially capable of producing $M_w \geq 7.2$ earthquakes. From a seismic hazard standpoint, one of the most critical questions about these faults concerns the frequency and size of future earthquakes that they might produce. For example, does the San Cayetano fault rupture in moderate-magnitude earthquakes similar to the 1994 M_w 6.7 Northridge and 1971 M_w 6.7 San Fernando-Sylmar earthquakes? If so, then the fault represents a hazard primarily to the local communities of the rapidly urbanizing Ventura Basin. Alternatively, does the fault rupture in its entirety in $M_w > 7$ events? Such large ruptures would affect a much larger area, including the densely populated San Fernando Valley, the cities of Ventura and Oxnard, and possibly the city of Los Angeles itself. A still more sobering scenario involves the potential for simultaneous rupture of the San Cayetano fault with other north-dipping reverse faults along strike to the east. Rupture of the entire 165 km-long Cucamonga-Sierra Madre-Santa Susana-San Cayetano system could produce a $M_w \geq 7.6$ to 7.7 earthquake (Dolan et al., 1995). Such an earthquake would cause catastrophic damage to a very large area encompassing the densely urbanized areas of the Los Angeles and Ventura basins. Thus, understanding the past behavior of the San Cayetano fault and the likelihood of a near-future earthquake are critical to assessing the short- and long-term seismic risk to a significant portion of southern California's population.

Investigations Undertaken

As part of an earlier NEHRP-funded paleoseismologic project, Dolan and Rockwell (2001) excavated a trench across the active trace of the eastern (Modelo) lobe of the San Cayetano fault, ~8 km east of the city of Fillmore and just west of the town of Piru, along the northern edge of the Ventura basin (Figure 2). This trench revealed evidence for a very young (1660-1813 A. D.) slip event that they interpreted as a large-magnitude earthquake on the San Cayetano fault, possibly the December 21, 1812 earthquake, or an event that occurred just before the beginning of the historic period (Dolan and Rockwell, 2001). Air photo and topographic map analysis indicates that the scarp that they trenched increases in height eastward from their trench site towards a maximum of 8 m high about 100 m to the east..

In an effort to determine a more precise age for the most recent event than could be determined by Dolan and Rockwell (2001) at their study site, as well as to attempt to determine the ages and displacements of older San Cayetano fault events, in 2002 my students and I excavated another trench (SCF2) across the tallest part of the scarp, ~100 m east of the Dolan and Rockwell (2001) trench. In addition, after backfilling the trench, we excavated three large-diameter boreholes through the back-filled SCF2 trench material and down into the deeper part of the section to determine the geometry of faulted

and folded strata at depths too deep for a trench exposure. These excavations form the focus of this report.

The SCF2 trench yielded displacement information from both the most recent event and the penultimate event (Figure 5). The trench contained abundant charcoal, as well as organic-rich buried soils, and we collected more than two dozen samples for analysis. We ultimately obtained Accelerator Mass Spectrometer (AMS) ^{14}C dates for 13 of these samples. Unfortunately, all of these samples appear to be reworked from older deposits. Nevertheless, we can place timing constraints on the two most recent surface slip events on the eastern section of the San Cayetano fault by comparing the stratigraphy revealed by the 2002 trench with the very similar stratigraphy seen in the earlier Dolan and Rockwell (2001) trench.

Non-Technical Summary

We excavated a trench and three large-diameter boreholes across the surface trace of the San Cayetano fault, a large, high-slip-rate reverse fault located near the northwestern corner of the Los Angeles metropolitan region. Our trench results show that within the past ~350 years the fault generated at least two very large (≥ 5 m) surface slip events. Our preliminary interpretation is that these represent large-magnitude (magnitude >7.0) earthquakes that probably ruptured the entire San Cayetano fault. Alternatively, Nicholson et al. (2007) has suggested that these slip events may record displacement on a very large, deep-seated (to 4 km depth) mega-landslide that they hypothesize extends along this part of the fault. However, there is no evidence that this mega-landslide is active, or capable of recurrent motion. Moreover, even if the slip events we observe are related to mega-slide movement, rather than direct earthquake surface rupture, the mega-slide probably only moves when activated by deep slip on the underlying fault. These results suggest that the recurrence interval between large San Cayetano fault earthquakes may be on the order of one to a few centuries, at least for the past two or three events. This observation is consistent with the very rapid slip rate inferred for this fault by previous researchers, and indicates that the San Cayetano fault represents a significant probabilistic seismic hazard to southern California.

Results

SCF2 trench site – During Summer 2002 we excavated a 32-m-long, 4.5- to 6-m-deep benched trench across the scarp of the Modelo lobe of the San Cayetano fault at what we refer to as our “SCF2” site (Figure 4). This site is located 2 km west-southwest of the city of Piru, and 8 km east of the city of Fillmore (Figures 1 and 2). The north end of the trench was located at 34.409386°N ; $-118.813381^\circ\text{W}$, and the south end of the trench was at 34.409074°N ; $-118.813378^\circ\text{W}$. The SCF2 trench was located ~100 m to the east of the Dolan and Rockwell (2001) trench site, along the same topographic scarp. Both trenches were excavated into deposits of a small alluvial fan emanating from the mouth of Edwards Canyon 500 m to the north of the trench site. For reference, the earlier trench site (which Dolan and Rockwell [2001] termed the “SCL” site), lies along the western edge of the same Edwards Canyon alluvial fan (Figure 2).

As part of our earlier efforts (Dolan and Rockwell, 2001) to locate suitable trench sites along the eastern (Modelo) lobe of the San Cayetano fault, we used aerial photographs and field reconnaissance to identify scarps. We then ruled out scarps that were clearly associated with recent erosion by the Santa Clara River. Beginning at the west edge of the town of Piru, a 5-m- to 8-m-tall, south-facing scarp extends west-southwestward for 3 km to near Hopper Canyon, where the scarp has been obscured by recent erosion and deposition along Hopper Creek (Figure 2). The trend of the scarp projects to the topographic mountain front west of Hopper Canyon. Between Piru and Hopper Creek, the scarp extends across several small alluvial fans of differing elevation without a significant change in scarp height, which suggested to us that it was of tectonic origin. This interpretation is also supported by the fact that active, south-flowing drainages in the area cross the scarp at near right angles. This feature was first identified by Çemen (1977; 1989), who described 'warping' of the alluvial fans south of the mountain front between Piru and Hopper Canyon.

The scarp at the SCF2 trench site is located ~100 m south of the topographic break in slope at the southern edge of the mountain front. To the east of the trench site, the scarp lies as much as 300 m south of the mountain front. The N70°E-trending scarp is ~5 to 8 m tall, and extends nearly continuously for ~3 km from the western edge of Piru to just east of Hopper canyon. The scarp is marked by abrupt topographic inflection points at its top and base. At the SCF2 trench location, the south-facing scarp slope is ~12°, whereas the ground surface to the north and south dips gently southward at $\leq 3^\circ$. The scarp at the SCF2 trench was 8 m tall, as measured across the displaced, gently south-dipping fan surface above and below the scarp. This is the tallest point on the scarp observed between Hopper Canyon and Piru.

Stratigraphy – The SCF2 trench and boreholes exposed a stratigraphic section that is remarkably similar to that exposed in the nearby Dolan and Rockwell (2001) trench (Figure 4). This is perhaps not surprising given the proximity of the two trenches (100 m apart), as well as the fact that they were both excavated into the same young (active) alluvial fan. Specifically, both trenches exposed well-bedded alluvial sands, silts, and pebble-cobble gravels, several of which could be traced the length of the trench exposure. To emphasize the similarity of these units in the two trenches, and to facilitate comparison between the SCF2 and earlier Dolan and Rockwell (2001) trench data, we here number the SCF2 units with the same unit numbers as the correlative units exposed in the Dolan and Rockwell (2001) trench.

For the SCF2 trench, all measurements described below are in meters north of the south end of the trench, followed by an elevation in meters relative to an arbitrary datum established near the ground surface of the southern end of the trench. For example, the ground surface at the north end of the trench, which is located 30.5 m north of the south end of the trench at an 'elevation' of plus (+) 5 m relative to our arbitrary datum, would be noted as m30.5N; +5.0 m.

We encountered seven major stratigraphic units in the trench, referred to as Units 1 through 8, from youngest to oldest; Unit 3 from the Dolan and Rockwell (2001) trench

was not encountered in SCF2, and Unit 8, the deepest unit exposed in SCF2 trench, was not exposed in the Dolan and Rockwell (2001) trench, which did not extend as deep. Unit 1, the youngest unit exposed in the SCF2 excavations, consists of predominantly sandy, well-bedded historical alluvium. The historical age of these deposits is demonstrated by the presence of a soda can (m23.8; +4.2m), and by several small pieces of plastic embedded in the deposit. The historical Unit 1 alluvium overlies Unit 2 along an irregular, bioturbated gradational contact.

In the SCF2 trench, Unit 2 is a wedge-shaped deposit limited to the southernmost part of the trench at the base of the scarp. This deposit consists of pale-yellow brown (2.5Y 5/5), friable, fine-grained sand with locally well-defined, thin bedding. In other locations, this internal bedding has been destroyed by the numerous rodent burrows that mark the upper part of the exposure. Unit 2 overlies Unit 4 along a sharp, generally planar contact, marked in most places by a 5-15-cm-thick basal sand. As noted above, Unit 3 of Dolan and Rockwell (2001) was not encountered in trench SCF2, presumably because this trench did not extend far-enough south to encounter the Unit 3 wedge at the extreme southern toe of slope.

Unit 4 is a medium-brown (10YR 3.5/3) poorly sorted, matrix-rich pebble to large cobble gravel. The matrix of the Unit 4 gravel is a silty sand. The unit is distinguished by its rather dark color, which we interpret as being due to development of a weak buried paleosol within the unit; no evidence for an incipient B horizon, either calcic or cambic, was apparent. Unit 4 is restricted to a southward-thickening, wedge-shaped deposit at the base of the scarp, leading us to interpret this as a colluvial wedge composed of material shed off the scarp, as discussed below.

Unit 5 is a pale yellow-brown (2.5 Y 5.5/4 to 10YR 5.5/5), pebble-small cobble gravel that can be traced for the entire length of the trench and borehole exposure. The unit exhibits a relatively constant thickness of 1.0-1.1 m north of m16, thickening gradually to as much as 2.5 m (measured perpendicular to bedding, including perhaps some thickening due to distributed shortening, as discussed below) at m11. The unit thins southward to ~1.6 m in borehole 3. The unit is distinguished from overlying Unit 4 predominantly on the basis of its paler color, a sandier matrix, and a larger percentage of clasts relative to matrix. Unit 5 overlies Unit 6 along a sharp, generally planar (but locally erosional; e.g., m15.5) contact

Unit 6 is a cohesive silt to silty fine-grained sand that locally contains ~10% disseminated small pebbles. This medium yellow-brown (10YR 4/4 to 2.5 YR 4.5/5) unit is locally well laminated on a centimeter scale. The cohesive nature and darker color of this unit lead us to interpret it as a weakly developed, buried A horizon. As with the Unit 4 paleosol, there is no indication of incipient development of any B horizon, either argillic or carbonate. North of m16.5, Unit 6 is 60-90 cm thick. The unit thickens gradually to ~1.8 m thickness between m11 and m13, and the upper and basal contacts diverge from one another. This divergence in dip suggests that Unit 6 was deposited as a wedge-shaped unit, perhaps at the base of a gentle paleo-scarp. South of the fault zone, unit 6 exhibits a relatively constant thickness of 70-90 cm in boreholes 1 and 2, again consistent with the

notion that the unit had a colluvial component of deposition, forming a thicker deposit at the base of a paleo-scarp. Unit 6 overlies Unit 7 along a sharp, slightly irregular to planar contact.

Unit 7 is a 2-m-thick sequence of generally thin-bedded (predominantly 1-20 cm thick) sands and pebble gravels. Contacts between individual beds are generally sharp, and there is local interfingering among beds. This unit was exposed in the bases of boreholes 1 and 2; borehole 3 did not penetrate deeply enough to expose this unit. Unit 7 overlies Unit 8 along a sharp contact marked by the presence of a basal-Unit 7 sand layer.

Unit 8, the lowermost unit exposed in the trench, is a brown (10YR 3.5/3) silty fine-grained to medium-grained sand, with local minor clay and small pebbles. The dark color of the unit suggests that it is the buried A horizon of a weakly developed paleosol similar to those we observed in unit 4 and 6. As in those younger paleosols, the Unit 8 soil exhibits no evidence of even incipient development of either a cambic or calcic B horizon.

Age Control – We collected several dozen detrital charcoal fragments from throughout the stratigraphic interval exposed in the SCF2 trench. From these, we obtained Accelerator Mass Spectrometer (AMS) radiocarbon dates on thirteen samples at the Lawrence Livermore National Lab Center for Accelerator Mass Spectrometry (CAMS). These data are presented in Table 1.

Unfortunately, there are major problems with inheritance in these data, as samples from the same layers yield widely divergent ages, and all of the SCF2 radiocarbon dates are much older than the age suggested for these deposits by the minimal soil development. This problem was also encountered in the earlier Dolan and Rockwell (2001) trench, and indicates extensive reworking and re-deposition of detrital charcoal from older deposits upstream in Edwards Canyon. Fortunately, the near-identical stratigraphic sections exposed in the two trenches allow us to use the few un-reworked dates from the Dolan and Rockwell (2001) trench to constrain the ages of the SCF2 deposits.

In the earlier Dolan and Rockwell (2001) trench, three radiocarbon samples were much younger (by thousands to tens of thousands of years) than other charcoal dates for the same layers. Although in some circumstances such dates would be interpreted as having been bioturbated into the deposit after deposition, several features suggested to those authors that these dates in fact represented the true depositional age of the sediments. First, the juxtaposition of samples of widely divergent age was a clear indication of at least some reworking from older deposits. This interpretation was also supported by the fact that in several cases the widely divergent ages from some deposits were all younger than equally widely divergent ages of samples from an overlying, clearly younger deposit. Moreover, the antiquity of many of the charcoal samples dated in both trenches (from 5 ka to >45 ka) is incompatible with evidence for minimal soil development. Specifically, the weak A/C profiles evident in the Unit 4, Unit 6, and Unit 8 paleosols, and in the active surface soil, with no evidence for the development of even incipient cambic (Bw) or calcic (Bk) B horizons, indicates relatively brief periods of soil

development on the order of hundreds, rather than thousands, of years. For example, the weak unit 4 soil is equivalent to the soils on Q2 deposits of Rockwell et al. (1985), which are typically less than 500 years old. Finally, there is the observation that the two best-constrained young dates from the earlier Dolan and Rockwell (2001) trench (their samples SCL-40 [calibrated age of A.D. 1660–1950] from unit 5, and SCL-44 [calibrated age of A. D. 1641-1950] from unit 3) were recovered from stratigraphically distinct layers that lacked any evidence for bioturbation (SCL-44 from the Unit 3 gravel and SCL-40 from a fine-grained, well-bedded silt layer within unit 5), making post-depositional introduction of these samples an unlikely explanation. Taken together, these observations led Dolan and Rockwell (2001) to interpret the stratigraphic section encompassing at least units 1 through 5 as having been deposited during the past few hundred years. This inference is supported by the A. D. 1478–1648 calendric age of sample SCL-13 from the Dolan and Rockwell (2001) trench. This sample, which was recovered from near the top of unit 6, yielded a slightly older age, as expected, than the sample SCL-40, which was recovered from younger Unit 5. The similarity of these two ages suggests that Units 5 and 6 were deposited within no more than a few hundred years of one another, and the ~200 year difference in the ages is consistent with the weak A/C soil profile developed within Unit 6 (Dolan and Rockwell, 2001).

We re-emphasize here the similarity of the stratigraphy exposed in the SCF2 trench to that exposed in the earlier Dolan and Rockwell (2001) trench. Given the distinctive nature of these strata, in terms of stratigraphic succession, sediment color and texture, bedding and sedimentary contact characteristics, and the degree and stratigraphic position of soil development, we think it highly unlikely that the deposits are significantly diachronous on the scale of the 100 m distance between the two trench sites.

In addition to the radiocarbon dates from the detrital charcoal samples, we have two other constraints on the age of the deposits. We recovered a soda can from the middle of Unit 1 on the east wall of the SCF2 trench (m23.26; +3.95 m). In the SCF2 trench, as in the earlier Dolan and Rockwell (2001) trench, Unit 1 is characterized by a dark brown, active A horizon developed through the historical deposits. The absence of a discernible cambic (Bw) horizon, or extensive pedogenic carbonate suggests to us that the surface soil records only a minimal period of soil development. This weakly developed A/C profile is equivalent to Q2 deposits of Rockwell et al. (1985), which are typically <500 years in age. As noted above, Units 4, 6, and 8 exhibit similar, weakly developed buried A/C profiles, and thus also probably record brief periods of soil development. The absence of any evidence for extensive soil development leads us to infer that the stratigraphic section exposed in the trench is latest Holocene in age.

We also attempted to determine whether there were traces of European-introduced pollen in the sediments. The presence of such pollens would help us to determine more precisely the age of the most-recent slip event. Most especially, we hoped to determine whether this event could have been the historic December 21, 1812 earthquake, as suggested by Dolan and Rockwell (2001). Accordingly, we shipped several samples to Roger Byrne at UC Berkeley Quaternary Paleoecology Laboratory for preliminary analysis. Unfortunately, Professor Byrne and his students determined that there was no pollen

present in these samples. Apparently any pollen that was deposited with these sediments had subsequently been oxidized during burial.

Evidence for Faulting--The trench exposed four major faults, which we refer to as faults F1 through F4, from north to south (Figure 4). Each of these faults might actually be more properly referred to as a fault zone, as each exhibits multiple, locally anastomosing strands, as well as evidence for local areas of distributed shearing and thickening. The four major fault zones exhibit a southward-decreasing fanning of dips. Fault F1 dips 30°N , fault F2 dips $\sim 28^{\circ}\text{N}$, fault zone F3 dips $\sim 25^{\circ}\text{N}$, and fault F4 dips $\sim 18\text{-}20^{\circ}\text{N}$. This geometry suggests that these various strands merge together downdip just below trench depth.

Restoration of the top and base of Unit 4 across all of these strands indicates that the most-recent event generated ~ 5 m of total fault slip. These strands cut up to within a few centimeters of the ground surface and displace all units except the Unit 1 historical alluvium. The erosional base of Unit 1 truncates fault strands 1 and 2; Unit 1 does not extend to the base of the scarp, and fault zones 3 and 4 terminate within the uppermost exposed part of Unit 2 just below the ground surface, within the active A horizon of the surface soil.

As shown in figure 5, back-slipping the fault zone by 5 m restores both the top and base of the wedge-shaped Unit 4. Interestingly, restoration of 5 m of reverse slip on the four main fault zones also restores the deposits below the Unit 4 wedge into laterally continuous units, indicating that brittle slip in the most-recent event (MRE) has affected all units exposed in the trench and boreholes by the same amount, confirming that this displacement occurred during a single event. However, the units below the Unit 4 wedge do not restore to a relatively planar, gently south-dipping geometry as would be expected if they had been deposited on the gentle fan surface (or a gentle pre-existing scarp – see discussion below), and had been deformed only in the MRE. Rather, on the MRE-restoration, Units 5 and below exhibit a pronounced fold with a near-vertical forelimb across the lower part of the fault zone near fault zone 4 (Figure 5). These observations demonstrate that the older units (Unit 5 and older) exposed in the SCF2 excavations have been deformed by at least two major slip events, which we refer to as Event 1 (the most-recent event, or MRE) and Event 2, the penultimate event.

Estimating the amount of thrust slip required to generate the fold evident in units 5 and 6 in the MRE restoration (Figure 5) is somewhat complicated by the unknown depositional geometry of these units. Specifically, if Units 5 and 6 were deposited across the entire fault zone as planar sheets of relatively constant thickness at the very gentle gradient evident in the northernmost and southernmost parts of these units exposed north of m23 in the trench and south of m8 in the borehole exposures, then “unfolding” of the fold revealed by the MRE restoration would require an extremely large amount of thrust displacement, on the order of 10.5 to 17.5 m, depending on the dip of the fault used (the range reflects the different dips of the four main faults, from 18° - 30°). This amount of slip seems extremely unlikely to have occurred in one event, especially in light of the very young age of these deposits. An alternative restoration that we think is much more

likely is based on the observation that the Unit 6 silt appears to thicken depositionally southward from ~m15, from ~60–90 cm to a maximum thickness of ~1.6 m south of m14. As with the northern part of Unit 6 in the trench exposure, the southernmost part of Unit 6 observed in the footwall of the fault zone in boreholes 1-3 exhibits a planar geometry and relatively constant thickness of ~70–90 cm. This geometry of Unit 6 across the fault zone suggests to us that unit 6 may have been deposited across a gentle pre-Event 2 scarp, with slight thickening of the unit as these sediments partially ponded near the base of the scarp. In this scenario, the 8° southward dip of the top of unit 6 between m13 and m22.5 reflects the depositional geometry of the unit, and provides a more-appropriate restoration horizon for determination of the total amount of slip necessary to generate the folding evident in the MRE restoration.

If we use this south-dipping contact as the restoration horizon for the hanging-wall, and the near-horizontal top of Unit 6 observed in the boreholes projects to the fault as the restoration horizon for the footwall block, the folding evident in Unit 6 could have developed with as little as ~ 5 m of thrust displacement. Thus, although thrust slip in the penultimate event could have been anywhere between as little as 5 m to as much as 17.5 m, we think that the geometry of Unit 6 probably indicates that it was deposited on a gentle slope across a low-relief scarp. This would suggest that the likely displacement in the penultimate slip event was nearer the low end of the possible range.

Discussion

The SCF2 excavations yield evidence for the two most recent slip events on the Piru strand of the eastern San Cayetano fault. Specifically, as described above, restoration of 5 m brittle slip restores the shallower stratigraphic units, especially Unit 4, into a reasonable depositional geometry. This restoration also reveals evidence for the penultimate slip event, in the form of a pronounced fold affecting pre-Unit 4 strata across the fault zone. The wedge shape of the Unit 4 deposit leads us to interpret it as having been deposited as a colluvial wedge formed after the scarp-forming folding that occurred during the penultimate slip event. Slip in the penultimate event (Event 2) is more difficult to measure precisely. As described above, however, it was probably ~5 m, although it is possible that it may have been significantly greater. Whatever the exact slip in Event 2, both of these slip events resulted in a large amount of surface reverse slip.

Although all of the 13 detrital charcoal samples that we dated turned out to be reworked, the similarity of the distinctive stratigraphy exposed in the SCF2 trench and the Dolan and Rockwell (2001) trench gives us confidence that the ages recovered from the earlier trench can be extrapolated to constrain the slip events we observe in the SCF2 trench. Moreover, the extrapolated ages from the earlier trench site are supported by the minimal level of soil development in SCF2, which suggests that the stratigraphic section exposed in that trench is latest Holocene in age. These ages indicate that both slip events that we see at the SCF2 trench have occurred since 1660 A. D. Thus, inasmuch as Dolan and Rockwell (2001) argued that the probable most-recent-possible age for the MRE at the west Piru site is December 21, 1812 (the date of the most recent large earthquake in the

region), the two SCF2 slip events appear to have occurred during an ~150-year-long interval between 1660 and 1813 A. D.

Dolan and Rockwell (2001) interpreted the most recent slip event at their west Piru trench as a large-magnitude ($M_w \geq 7.5$) earthquake, possibly the destructive December 21, 1812 earthquake, which caused damage throughout the western Transverse Ranges. This slip event is the same slip event we observe in the SCF2 trench, and in both trenches this event resulted in ~ 5 m of reverse displacement. As discussed below, however, the tectonic significance of these slip events may be more complicated than inferred by Dolan and Rockwell (2001).

Structure contour maps of the fault surface reveal that the SCF exhibits an anomalous, “scallop-shaped” fault configuration beneath the Modelo lobe (Çemen, 1977; 1989; Yeats and Huftile 1995a). Specifically, the deeper parts of the fault dip moderately to steeply north, but the fault dip becomes gentler towards the surface to $\leq 20^\circ$ beneath the trench (e.g., Yeats and Huftile, 1995b). Nicholson et al. (2007) proposed the intriguing possibility that the scallop-shaped Modelo lobe section of the San Cayetano fault formed during a mega-landslide involving more than 60 km³ of material, and extending as deep as 4 km below ground surface. The evidence they presented is certainly consistent with a mega-slide, and emplacement of such a deep-seated landslide may explain the origin of the gentle dip of the upper part of the San Cayetano fault. We note, however, that the Nicholson et al. (2007) cross section does not appear to have been corrected for apparent-dip effects caused by the irregular trace of their cross-section line, resulting in a misleading listric geometry for the fault surface (see Çemen [1989]; Yeats et al., [1994]; and Huftile and Yeats [1995b; 1996] for sections that do not suffer from this problem). Thus, although the fault does roll over to a gentler dip in the upper few kilometers, and especially in the uppermost kilometer, the effect is not as extreme as that portrayed in Nicholson et al. (2007). It is important to note, however, that even if the mega-landslide exists, neither its state of activity, nor the possibility of recurrent slip, have been documented. Although the evidence presented by Nicholson et al. (2007) strongly suggests a mega-landslide origin for the Modelo lobe, and for the gentler near-surface dip of the eastern segment of the San Cayetano fault, there is no evidence that the mega-slide is an active feature. Indeed, as pointed out by Nicholson et al. (2007) themselves, “...the slide mass appears relatively stable though [sic]” (caption to their figure 13E). Thus, there is no reason to suppose that the mega-slide has moved (or is even capable of moving) since its initial emplacement, which remains undated.

Nicholson et al. (2007), however, tacitly assume that the slide is active and capable of recurrent motion, and they suggest various scenarios involving reactivation of the mega-slide that might obviate the use of surface slip data from the trenches as evidence for direct tectonic slip. Two of their possible scenarios (scenarios B and D) involve co-seismic slip on the deep parts of the fault that either (B) does not extend all the way to the surface, or (D) extends upward into the hangingwall block well to the north of the surface scarp we trenched. Both of these possibilities would require that this deformation be manifested at the surface after several such events. This does not appear to be the case, and we therefore consider these possibilities to be extremely unlikely. Their possibility E

involves independent (i.e., not San Cayetano fault-related) slip of the mega-slide triggered by increased fluid pressure and/or strong ground shaking in a nearby earthquake. Although this possibility cannot be ruled out, the idea that such a large-volume, deep-seated slide could move numerous times without being triggered by seismic rupture of the underlying San Cayetano fault also seems highly unlikely. The two remaining possibilities, A and C, thus appear to be most plausible of the options suggested by Nicholson et al. (2007). Both of these scenarios involve co-seismic slip on the deep parts of the San Cayetano fault that either (A) extends all the way to the surface scarp we trenched, or (C) triggers movement of the mega-slide, including slip on the shallowest part of the fault, which coincides with the basal detachment of the mega-slide and reaches the surface at the SCF2 trench site.

If activity and recurrent motion of the mega-landslide proposed by Nicholson et al. (2007) can be established, then these authors would indeed be correct in noting that displacements measured at the surface trace of the San Cayetano fault may not be indicative of true co-seismic slip, and thus should not be used to infer magnitudes of paleo-San Cayetano fault earthquakes, as was done by Dolan and Rockwell (2001). However, in the absence of evidence for recent and recurrent activity on the mega-slide, we think that the displacements measured at the San Cayetano fault excavations reported herein and by Dolan and Rockwell (2001) probably do represent tectonic fault slip. Moreover, one of the points of the Nicholson et al. (2007) study is that the complex near-surface geometry for the fault proposed in their cross section, with a listric flattening and even local reversal of dip in the near-surface, makes it extremely unlikely to rupture dynamically, even during a large-magnitude rupture on the underlying San Cayetano fault. As noted above, however, the geometry shown in their cross section (their figure 2) seems to include apparent-dip effects related to the irregular trace of their cross-section line, including at least one section that appears to extend at a relatively low angle to the fault trace (we note, however, that due to the very small print size of their location map, it is extremely difficult to precisely locate the wells used to construct their cross section). In contrast, the geometry of the shallow parts of the San Cayetano fault shown in the cross sections of Çemen (1977; 1989), Yeats et al. (1994), and Huftile and Yeats (1995b; 1996), which do not suffer from apparent-dip effects, is much more planar, allowing for more likely propagation of a dynamic rupture all the way to the surface trace of the fault during large-magnitude San Cayetano fault earthquakes.

If the large displacements that we measure in the SCF2 trench for the two most recent slip events do represent true co-seismic displacements, and not slip at the toe of the proposed mega-landslide, then the earthquakes that generated these slip events were likely of large magnitude ($M_w > 7$). Such large-magnitude events would likely have involved rupture the San Cayetano fault in its entirety, possibly together with adjacent faults, such as the blind Sisar detachment system to the west (Huftile and Yeats, 1995a) and/or the Santa Susana system to the east (Yeats, 1987).

In contrast to the surface displacements we measure, the timing of the two most recent slip events is somewhat less controversial. Given the remarkable similarity in the stratigraphic sections observed in the SCF2 excavations and the earlier Dolan and

Rockwell (2001) trench, we feel confident in extrapolating the radiocarbon age constraints from the Dolan and Rockwell trench to the SCF2 excavations discussed herein. These data suggest that both slip events occurred after the deposition of Unit 5, which occurred after the 1660 A. D. maximum age of a detrital charcoal sample recovered from that unit in the Dolan and Rockwell (2001) trench. Even if the age correlations between the two trenches are not exactly correct, and there was some diachronous deposition and soil development between the two trenches, the minimal soil development observed in the SCF2 excavations (as well as in the earlier Dolan and Rockwell trench) indicates that the stratigraphic section at our study site is latest Holocene in age. This observation independently supports the radiocarbon results.

Taken together, these observations indicate that the Modelo lobe of the San Cayetano fault has slipped at least twice since 1660 A. D., presumably in large-magnitude earthquakes, but possibly in response to slip on the proposed mega-slide (although we re-emphasize that there is no evidence for current or recent activity of this feature). Dolan and Rockwell (2001) suggested that the MRE observed in their trench was either the damaging December 21, 1812 earthquake, or an event that occurred just before the historic era. To the best of our knowledge, there are no other potential candidate large-magnitude earthquakes in the western Transverse Ranges (e. g., Topozada et al., 1981). Thus, the two slip events we observe in the SCF2 excavations appear to have occurred between 1660 and 1813. Moreover, as noted above, the geometry of Unit 6 in the SCF2 excavations strongly suggests that it was deposited above a pre-existing scarp, which must have been generated in the ante-penultimate event (Event 3). This scarp would have developed during Unit 7 or Unit 8 time. As with the rest of the stratigraphic section exposed in both the SCF2 and earlier SCL excavations, the minimal soil development observed in SCF2 units 6 and 8 suggests that this section was probably deposited rapidly. These observations suggest that possible-Event 3 is also of latest Holocene age. The lone radiocarbon date recovered from Unit 7 that is not obviously reworked is SCL-3, from near the base of Unit 7 in the Dolan and Rockwell (2001) trench. The 3080-2038 B.C. calibrated age range (i.e., 5080-4038 cal yBP relative to 2000 A. D.) reported for this sample thus provides an absolute maximum age for possible-Event 3, although we reiterate that because of the extensive reworking of charcoal in both trenches, and the observations of minimal soil development, we suspect that the actual age of Unit 7 (and therefore of possible-Event 3) is much younger than the SCL-3 age range. Thus, the San Cayetano fault has generated at least two, and probably three, slip events during latest Holocene time. These short return times suggest that the San Cayetano fault generates earthquakes of sufficiently large magnitude to cause major surface deformation (in the form of either true co-seismic surface slip, or triggered slip of the mega-landslide proposed by Nicholson et al. [2007]) on the time scale on the order of one to a few centuries, at least for the past two or three events. This observation is generally consistent with the very rapid slip rate for the eastern lobe of the fault (10-12 mm/yr; Yeats, 1993; Huftile and Yeats, 1996) and with geodetic evidence for very rapid strain accumulation (e.g., Donnellan et al., 1993a; 1993b; Hager et al., 1999), and suggests that the San Cayetano fault represents a major probabilistic hazard to southern California. We note, however, that if the slip events we observed in the trenches record true co-seismic displacement, the 10 m of minimum slip observed since 1660 A. D. suggests a slip rate

that is faster than the long-term rate along the fault. This suggests that if the slip events we measure in the excavations are large-magnitude San Cayetano fault earthquakes, the fault may be experiencing a cluster of activity that is not reflective of its long-term average behavior. Alternatively, if the surface displacements do not reflect true tectonic slip, but rather some combination of seismic slip and landslide movement, then the recurrence data could be consistent with the frequent occurrence of smaller-magnitude events on the San Cayetano fault. If this second possibility were true, however, these events would have to be of sufficiently large magnitude to trigger slip on the mega-landslide.

Acknowledgments

I am grateful to USC graduate students Ross Hartleb, Ken Austin, Scott Marsic, and Shari Christofferson, and USC undergraduates Marcos Marin, Jeff Hoeft, Kyle Sherk, Kristen Kiker, and Michael Getman for their help with the excavations. I would also like to thank Tom Rockwell for helpful discussions and Roger Bryne and his students for their attempts to isolate pollen from the SCF2 paleosols.

References

- Bronk Ramsey, C., 2009, Bayesian analysis of radiocarbon dates OxCal: *Radiocarbon*, v. 51, 1, p. 337-360.
- Çemen, I., 1977, Geology of the Sespe-Piru Creek area, Ventura County, California: unpubl. M. S. thesis, Ohio University, Athens, Ohio, 69p.
- Çemen, I., 1989, Near-surface expression of the eastern part of the San Cayetano fault: A potentially active thrust fault in the California Transverse Ranges: *Jour. Geophys. Res.*, v. 94, p. 9665-9677.
- Dibblee, T. W., Jr., 1987, Geologic Map of the Ojai Quadrangle, Ventura County, California: *Dibblee Geol. Foundation Map #DF-13*, Santa Barbara, California (1:24,000).
- Dibblee, T. W., Jr., 1990a, Geologic Map of the Fillmore Quadrangle, Ventura County, California: *Dibblee Geol. Foundation Map #DF-27*, Santa Barbara, California (1:24,000).
- Dibblee, T. W., Jr., 1990b, Geologic Map of the Santa Paula Peak Quadrangle, Ventura County, California: *Dibblee Geol. Foundation Map #DF-26*, Santa Barbara, California (1:24,000).
- Dibblee, T. W., Jr., 1991, Geologic Map of the Piru Quadrangle, Ventura County, California: *Dibblee Geol. Foundation Map #DF-34*, Santa Barbara, California (1:24,000).
- Dolan, J. F., Sieh, K., Rockwell, T. K., Yeats, R. S., Shaw, J., Suppe, J., Huftile, G., and Gath, E., 1995, Prospects for larger or more frequent earthquakes in greater metropolitan Los Angeles, California: *Science*, v. 267, p. 199-205.

- Dolan, J. F., and Rockwell, T. K., 2001, Paleoseismologic evidence for a very large (Mw>7), recent surface rupture on the eastern San Cayetano fault, Ventura County, California: Was this the source of the damaging December 21, 1812 earthquake?: *Bull. Seismol. Soc. Amer.*, v. 91, p. 1417-1432.
- Donnellan, A., Hager, B. H., and King, R. W., 1993a, Rapid north-south shortening of the Ventura basin, southern California: *Nature*, v. 366, p. 333-336.
- Donnellan, A., Hager, B. H., King, R. W., and Herring, T. A., 1993b, Geodetic measurement of deformation in the Ventura basin, southern California: *Jour. Geophys. Res.*, v. 98, p. 21727-21739.
- Hager, B. H., G. A. Lyzenga, A. Donnellan, and D. Dong (1999), Reconciling rapid strain accumulation with deep seismogenic fault planes in the Ventura Basin, California: *Jour. Geophys. Res.*, 104, 25,207–25,219.
- Huftile, G. J., and Yeats, R. S., 1995a, Convergence rates across a displacement transfer zone in the western Transverse Ranges, Ventura Basin, California: *Jour. Geophys. Res.*, v. 100, p. 2043-2067.
- Huftile, G. J., and Yeats, R. S., 1995b, Cenozoic structure of the Piru 7 1/2-minute quadrangle, California: *U. S. Geol. Surv. Open-File Report 95-68*, Map Scale 1:24,000, 33 p.
- Huftile, G. J., and Yeats, R. S., 1996, Deformation rates across the Placerita (Northridge Mw 6.7 aftershock zone) and Hopper Canyon segments of the western Transverse Ranges deformation belt: *Bull. Seismol. Soc. Amer.*, v. 86, p. S3-S18.
- Nicholson, C., Kamerling, M. J., Sorlien, C. C., Hopps, T. E., and Gratier, J.-P., 2007, Subsidence, compaction, and gravity sliding: Implications for 3D geometry, dynamic rupture, and seismic hazard of active basin-bounding faults in southern California: *Bull. Seismol. Soc. Amer.*, v. 97, p. 1607-1620, doi: 10.1785/012006236.
- Reimer, P. J., and 27 others (2004), Radiocarbon calibration from 0-26 cal kyr BP – IntCal04 terrestrial radiocarbon age calibration, 0-26 kyrBP: *Radiocarbon*, 46, 1029-1058.
- Rockwell, T. K., Johnson, D. L., Keller, E. A., and Dembroff, G. R., 1985, A late Pleistocene-Holocene soil chronosequence in the central Ventura Basin, southern California, USA: in K. Richards, R. Arnette, and S. Ellis (eds.), *Geomorphology and Soils*, George Allen and Unwin, London, England, p. 309-327.
- Rockwell, T., 1988, Neotectonics of the San Cayetano fault, Transverse Ranges, California: *Geol. Soc. Amer. Bull.*, v. 100, p. 500-513.
- Schleuter, J. C., 1976, Structure of the Upper Ojai-Timber Canyon area, Ventura County, California, unpubl. M. S. thesis, Ohio University, 67p.
- Suppe, J. and Medwedeff, D. A., 1990, Geometry and kinematics of fault-propagation folding: *Ecolg. Geol. Helv.*, v. 83, p. 409-454.
- Topozada, T. R., Real, C. R., and Parke, D. L., 1981, Preparation of isoseismal maps and summaries of reported effects for pre-1900 California earthquakes: *Calif. Div. Mines Geol. Open-File Report 81-11*, Sacramento, CA.

Yeats, R. S., 1987, Late Cenozoic structure of the Santa Susana fault zone: *U. S. Geol. Surv. Prof. Paper 1339*, p. 137-160.

Yeats, R. S., 1993, Converging more slowly: *Nature*, v. 366, p. 299-301.

Yeats, R. S., Huftile, G. J., and Stitt, L. T., 1994, Late Cenozoic tectonics of the east Ventura basin, Transverse Ranges, California: *Amer. Assoc. Petrol. Geol. Bull.*, v. 78, p. 1040-1074.

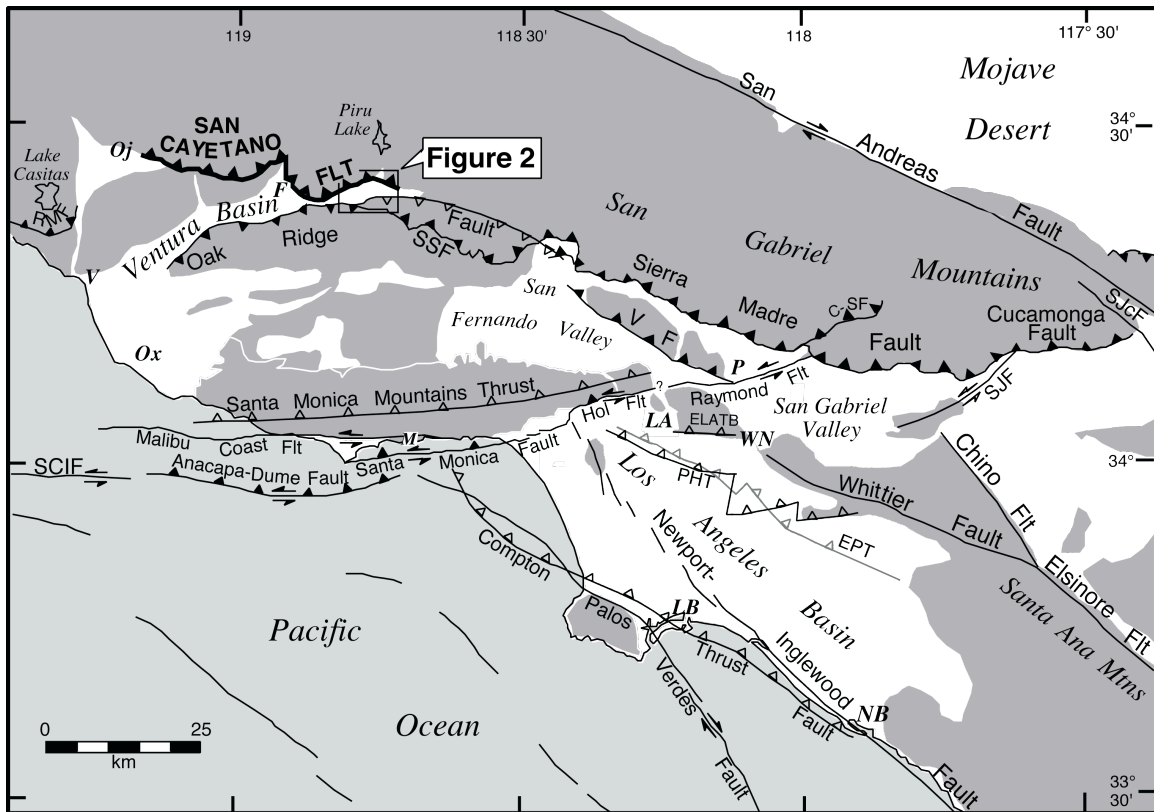


Figure 1. Regional neotectonic map for metropolitan southern California showing major active faults. The San Cayetano fault is a 40-km-long active reverse fault that extends along the northern edge of the Ventura basin, northwest of the Los Angeles metropolitan region (after Dolan and Rockwell, 2001). Closed teeth denote reverse fault surface trace; open teeth show upper edge of blind thrust fault ramps. Strike-slip fault surface traces shown by double arrows. C-SF = Clamshell-Sawpit fault; ELATB = East Los Angeles blind thrust system; EPT = Elysian Park blind thrust fault; Hol Flt = Hollywood fault; PHT = Puente Hills blind thrust fault; RMF = Red Mountain fault; SCIF = Santa Cruz Island fault; SSF = Santa Susana fault; SJcF = San Jacinto fault; SJF = San Jose fault; VF = Verdugo fault; F = Fillmore; LA = Los Angeles; LB = Long Beach; M = Malibu; NB = Newport Beach; Oj = Ojai; Ox=Oxnard; P = Pasadena; V = Ventura; WN = Whittier Narrows. Dark shading denotes mountains. Note location of figure 2.

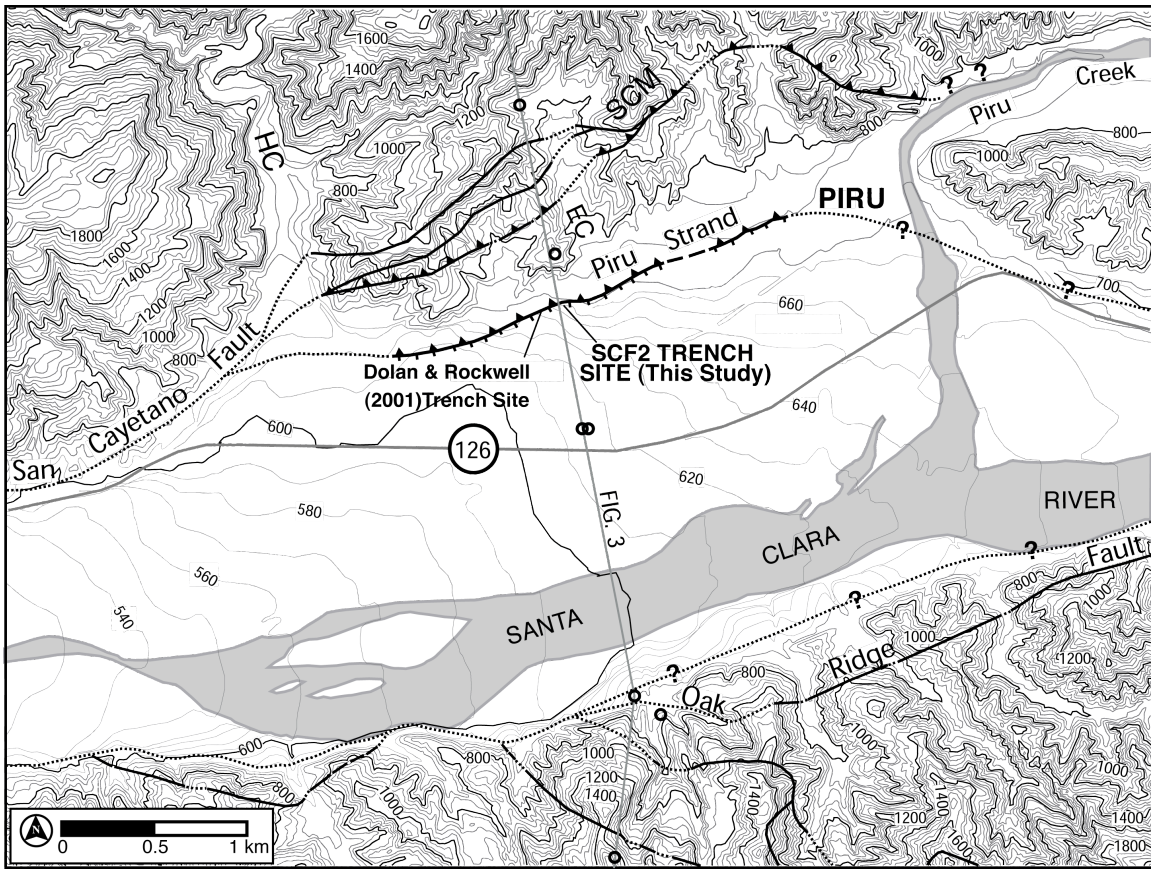


Figure 2. Map of the easternmost 6 km of the San Cayetano fault surface trace near the town of Piru (location in figure 1). Note location of the SCF2 excavations (the focus of this report) as well as the earlier trench of Dolan and Rockwell (2001) along the south-facing scarp of Piru strand of San Cayetano fault (scarps denoted by tick marks on downhill side). Reverse faults denoted by closed teeth on hanging wall. Traces of San Cayetano and Oak Ridge faults are from Dibblee (1991) except as noted. Trace of Piru strand of San Cayetano fault west of Piru is based on our air photo analysis and field work, following initial identification of these scarps by Çemen (1977; 1989). SCM is "main" strand of San Cayetano fault (terminology of Çemen, 1977; 1989; and Huftile and Yeats, 1995b), which we suspect may be inactive because this strand exhibits no clear-cut geomorphic evidence of recent activity (see text for discussion). Black open circles show locations of oil wells used to construct cross section shown in Figure 3 (Çemen, 1977; 1989; Huftile and Yeats, 1995b). EC = Edwards Canyon. HC = Hopper Canyon. Circled "126" shows State Highway 126. Buried, northernmost strand of Oak Ridge fault shown near southeast corner of figure is based on the observation of apparently uplifted Saugus Formation rocks north of the northernmost trace mapped by Dibblee (1991). Topography digitized from 1952 (photo-revised 1988) U. S. Geological Survey 1:24,000 scale Piru 7.5' Quadrangle. Topographic contour interval is 40' (12.2 m) in steep terrain; selected 10' (3.04 m) contours are shown in flatter areas.

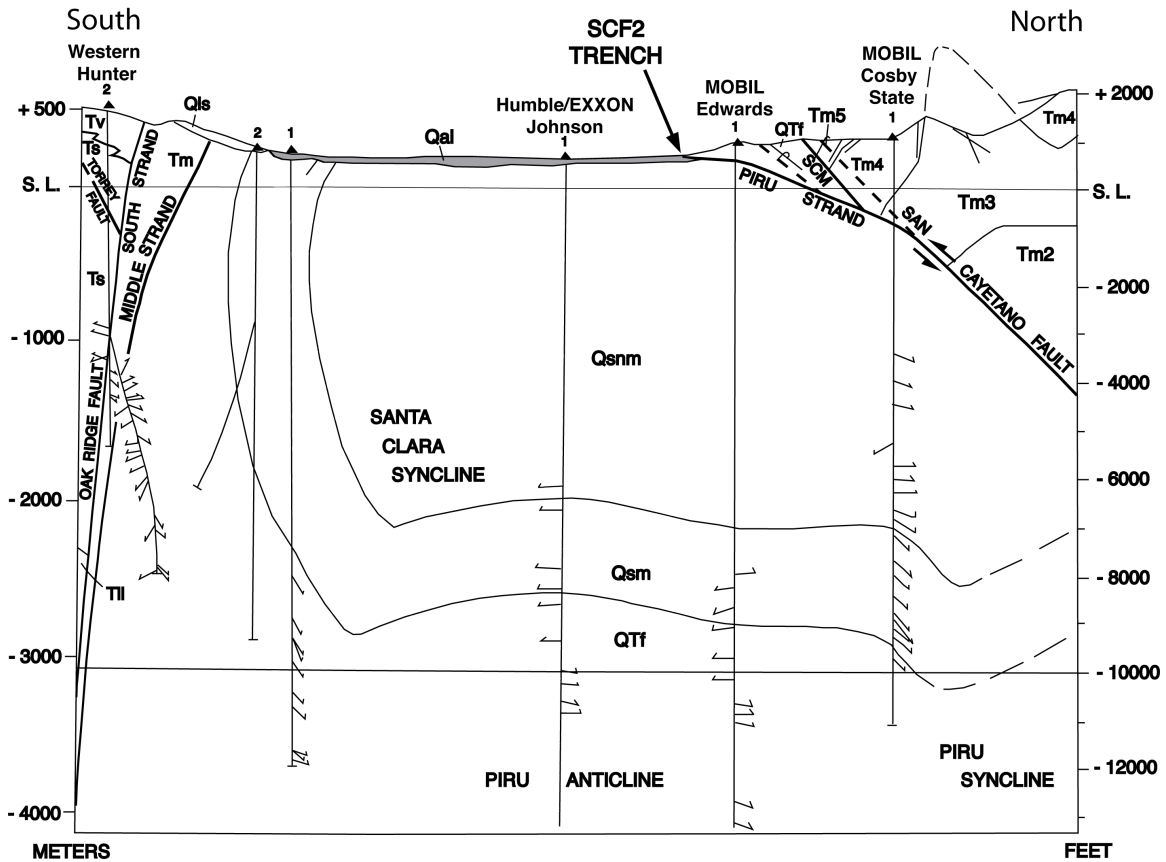


Figure 3. N10W cross section across the east Ventura Basin showing upper part of San Cayetano fault zone in the vicinity of our 1999 west Piru trench (from Çemen, 1977; 1989; and Huftile and Yeats, 1995b). See figure 2 for location. Thin, vertical lines are oil wells showing dip-meter data. Note near-surface splaying of San Cayetano fault into several distinct strands -- the more northerly "Main" strand of the San Cayetano fault (labeled "SCM" in figure), and the southern "Piru strand" (terminology of Çemen, 1977; 1989; and Huftile and Yeats, 1995b). We have modified the cross section to show the Piru strand reaching the surface at the SCF2 trench exposure, which results in a shallower near-surface dip than shown in Çemen (1989) and Huftile and Yeats (1995b). We have also added the two strands above and below the "Main strand" of the fault (shown by dashed lines) on the basis of mapping by Dibblee (1991). Qsm = Quaternary (Pleistocene) Saugus Formation, marine facies; Qsnm = non-marine facies of Saugus Formation. QTf = Quaternary-Tertiary (Mio-Pliocene) Towsley Formation. Tm1-5 = various members of Tertiary (Miocene) Modelo Formation.

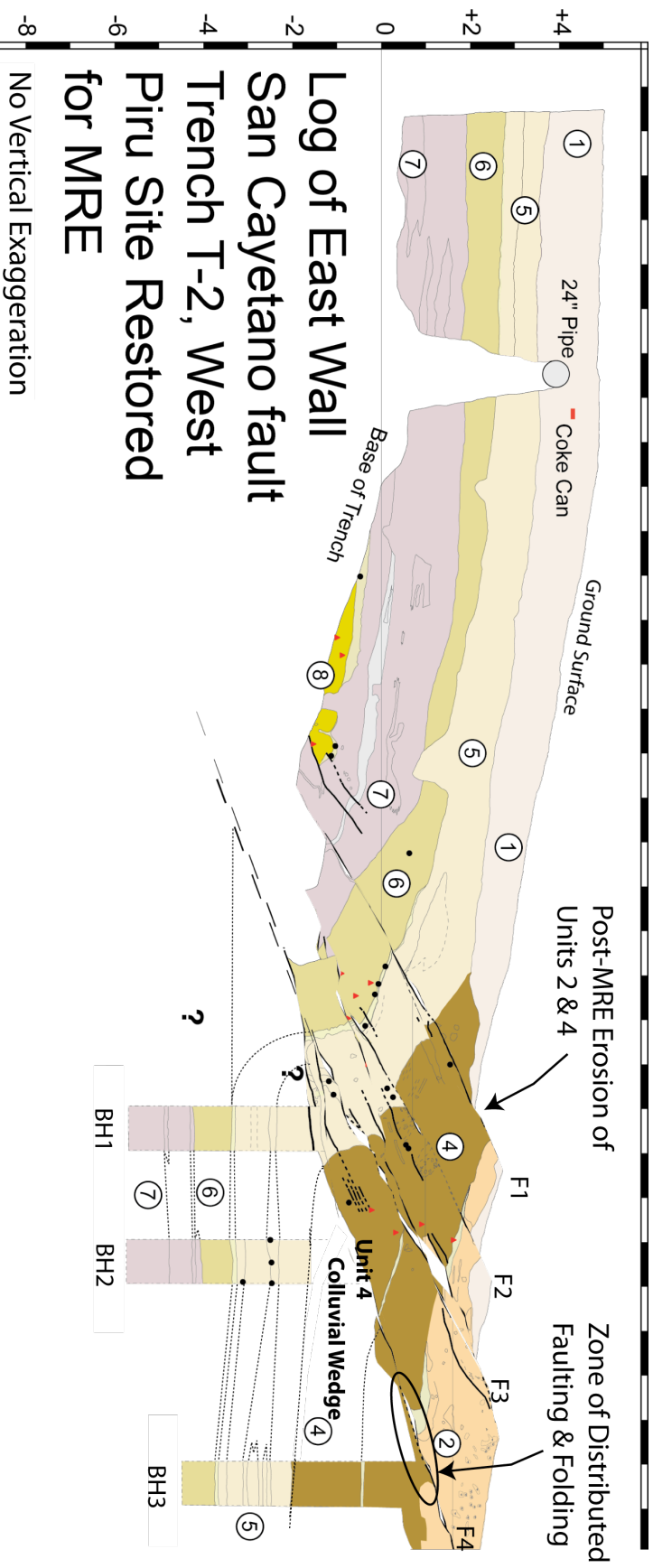


Figure 5. Log of east wall of SCF2 trench and boreholes back-slipped by 5 m to restore the pre-most recent event geometry of the stratigraphic units. See text for discussion. All other features same as figure 4.

Table 1. Radiocarbon ages for San Cayetano fault trench SCF-2.

CAMS #	Sample #	Unit #	Trench coordinates	¹⁴ C Age (yBP)	Calendric Age (cal yBP)
130487	SCF2-2	7 (base)	15.95; -1.11	9265 ± 45	10570-10286 (95.4%)
130488	SCF2-5	5	11.54; -2.76	8690 ± 80	10116-10071 (1.9%) 9922-9526 (93.5%)
130489	SCF2-6	6 (top)	10.98; -1.09	5605 ± 40	6467-6302 (95.4%)
130490	SCF2-7	7	27.05; +0.82 (west wall)	47,800 ± 1600	beyond calibration
130491	SCF2-8	6	12.36; -0.65	4570 ± 35	5445-5412 (8.3%) 5325-5258 (39.5%) 5249-5232 (1.6%) 5225-5214 (1.3%) 5189-5053 (44.7%)
130492	SCF2-15	7 (base)	18.65; -0.55 (west wall)	26,800 ± 840	beyond calibration
130493	SCF2-16	7 (base)	20.30; +0.80	>33,400	beyond calibration
130494	SCF2-18	4	8.74; -0.41	12,890 ± 100	15,608-14,921 (95.4%)
130495	SCF2-19	4	8.54; -0.40	25,040 ± 200	25450-24650 (95.4%)
130496	SCF2-22	6 (top)	11.60; -0.87	7300 ± 40	8180-8020 (95.4%)
130497	SCF2-BH2-24.5'	5	24.5' (7.47 m) depth	29,090 ± 450	beyond calibration

All samples are assumed to have a $\delta^{13}\text{C}$ value of -25 according to Stuiver and Polach (1977). Ages in radiocarbon years are based on Libby half-life of 5568 years following the conventions of Stuiver and Polach (1977). All samples were collected from the east wall of the SCF2 trench with the exception of SCF2 - 7 and SCF2- 15, which were collected from the west wall, and SCF2 - BH2-3 - 24'5", which was collected from borehole BH2 at a depth of 24' 5" feet (7.44 m).

All samples calibrated with OxCAL 4.1.3 (Bronk-Ramsey, 2009; using Reimer et al., 2004 [INTCAL04])